VALIDATION AND ANALYSIS OF LINEAR DISTILLATION MODELS FOR CONTROLLER DESIGN

Michael Amrhein*
Institut d'Automatique
Ecole Polytechnique
Fédérale de Lausanne
CH–1015 Lausanne
Switzerland

Frank Allgöwer†
Institut für Systemdynamik
und Regelungstechnik
Universität Stuttgart
D–7000 Stuttgart 80
F.R.G

Wolfgang Marquardt*
Lehrstuhl für Prozeßtechnik
Rheinisch–Westfälische
Technische Hochschule Aachen
D–5100 Aachen
F.R.G.

Keywords: model validation; singular directions; dynamic RGA; distillation control; H_∞–control

1 Introduction

The requirement for dynamic models for simulation is to describe a given process with the highest accuracy possible. On the contrary, a good model *for controller design* gives the *simplest* description of the process that captures the essential characteristics relevant for controller design. Despite the many advances in nonlinear control theory and its successful applications to chemical processes, i.e., including distillation control, linear controller design methods are further developed and more widely accepted than nonlinear techniques. In many cases linear models of low order suffice to describe processes accurately enough [3, 6, 12]. This paper is concerned with tools for analyzing and validating *linear* process models prior to controller design.

There are two main reasons for evaluating models for controller design. First, there is a necessity for model validation: we should check whether the model characteristics conform with those of the real process relevant to control. Secondly, analysis of the model gives information about achievable closed loop performance and hints on how to design a controller.

Usually, there are several models available. Identification, linearization, or other approaches yield models with, in general, different characteristics for the same process. It is a nontrivial task to decide whether a model describes the main dynamic characteristics of a process and to determine which model is to be preferred for controller design. Techniques for examining linear models for controller design are described in Section 2. One focus of this paper is on tools for analyzing multivariable processes in the frequency domain, for example, condition number and dynamic relative gain array (RGA) analysis. The latter tool is extended by the phase information of the RGA. A novel evaluation tool involving the singular directions over frequency of the respective processes is introduced.

Although simplified modeling of distillation columns for controller design has a long tradition (i.e., [3, 8, 12]), there is still a need for appropriate low–order models. In Section 3, a new linear low–order model is compared to five models from the literature [5] using the analysis tools introduced in Section 2. The new model directly exploits wave propagation phenomena, and, therefore, will be called the *wave model*. For details on the modeling approach used for this model we refer to [10]. Exemplary, a binary high purity distillation of an ideal mixture in a 40 tray column [12] is considered. We refer to it as column A in accordance with the original reference.

Finally, Section 4 shows briefly results of the H_∞-controlled column where the controller is designed on the basis of the wave model. Simulations with a detailed nonlinear distillation model show that very good control action can be achieved with this model. Moreover, the linear model allows to predict the nonlinear closed loop behavior quite accurately.

2 Validation and analysis tools

Techniques for evaluating linear models can be classified into time domain methods (e.g., pole/zero/gain–analysis or inspection of the prediction quality through time domain simulations) and frequency domain methods. As a direct consequence of the intended purpose of the model, i.e. controller design, analysis does not focus on the behavior of states, but rather on input/output behavior. For linear systems I/O analysis can be best performed in the frequency domain.

For SISO–systems the full I/O–information of a dynamic system is contained in its Bode diagrams, Nyquist diagrams, Nichols charts etc. The diagrams can be compared to the *measured* frequency response of the real system. Knowing the approximate envisaged bandwidth of the closed loop, good correspondence of model and real plant are only required for frequencies up to the bandwidth. Unlike SISO–systems, traditional analysis tools for MIMO–systems, such as singular values, condition number, and relative gain array, give only partial I/O–information because of the lack of phase information. The analysis of directional information will partly overcome these difficulties.

The definition of the RGA for the stationary case goes back to Bristol [2]. Recently, the *dynamic* RGA was

*This work has been done while these authors were with the Institut für Systemdynamik und Regelungstechnik, Universität Stuttgart
†To whom all correspondence should be addressed:
phone +49-711-6856193, fax +49-711-6856371;
email: allgower@rus.uni-stuttgart.de

found to be a useful tool to describe the degree of interaction of the I/O–quantities over frequency. Usually, the *magnitude* of the complex RGA–elements are plotted over frequency leaving out the phase information. But in order to use the full performance of this tool one should also include the *argument* of each RGA–element. The (1,1)–element λ_{11} of the RGA is given by the ratio $\lambda_{11} = \frac{l^u_{11}}{l^y_{11}}$ with $l^u_{11} = \frac{\partial y_1}{\partial u_1}\Big|_{u_k=0_{k\neq 1}}$ and $l^y_{11} = \frac{\partial y_1}{\partial u_1}\Big|_{y_k=0_{k\neq 1}}$ where l^u_{11} is the gain between input 1 and output 1 with all other inputs fixed at its stationary values. The gain between input 1 and output 1 with all other outputs (ideally) regulated is called l^y_{11}. The phase $\Delta\varphi_\lambda$ of the RGA is taken as the phase difference between the output signals in the case of the unregulated and regulated other outputs:

$$\Delta\varphi_\lambda = \varphi_{l^y_{11}} - \varphi_{l^u_{11}}$$

This characterisation can be used to measure the RGA of nonlinear systems.

Usually, only singular value diagrams of the multivariable processes are examined in order to characterise the I/O–behavior. This can however be very misleading. Two systems having exactly the same singular values over frequency can possess completely different dynamic features, especially if the system is ill–conditioned. We therefore suggest to use not only the singular values σ_i but also the directional information contained in the unitary, frequency dependent matrices $\mathbf{W}$ and $\mathbf{V}$ of the singular value decomposition (SVD):

$$\mathbf{y}(j\omega) = \mathbf{V}(j\omega)\mathbf{\Sigma}(j\omega)\mathbf{W}^H(j\omega)\,\mathbf{u}(j\omega) \qquad (1)$$

with $\mathbf{\Sigma}(j\omega) = \mathrm{diag}\{\sigma_i\}$ and $\bar{\sigma} > \sigma_2 \cdots > \underline{\sigma}$, $\mathbf{W} = [\bar{\mathbf{w}}, \mathbf{w}_2, \ldots, \mathbf{w}_{m-1}, \underline{\mathbf{w}}]$, $\mathbf{V} = [\bar{\mathbf{v}}, \mathbf{v}_2, \ldots, \mathbf{v}_{m-1}, \underline{\mathbf{v}}]$. Note that $\bar{(\cdot)}$ corresponds to the maximal and $\underline{(\cdot)}$ to the minimal singular value. We limit ourselves to square systems, although the method described below is valid for non–square systems, too. The matrices $\mathbf{W}$ and $\mathbf{V}$ can be interpreted from system theory: Consider the frequency ω^* to be fixed and suppose that $\mathbf{W}$ and $\mathbf{V}$ are real matrices. That is the case for systems without integral or derivative action and $\omega^* = 0$. This stationary case is intensively treated in [13]. In this work, however, $\mathbf{W}$ and $\mathbf{V}$ are examined over *frequency*. The first and last column of $\mathbf{W}$ contain important directional information in the input space and the first and last column of $\mathbf{V}$ contain important information in the output space. If the direction of the input vector $\mathbf{u}$ (*input–direction*) in the input space is parallel to the vector $\bar{\mathbf{w}}$ (*maximal input–direction*), this input signal will be maximally amplified by the system, i.e., by $\bar{\sigma}(\omega^*)$. The output will then point in direction of $\bar{\mathbf{v}}$ (*maximal output–direction*). The reasoning for $\underline{\mathbf{v}}$ and $\underline{\mathbf{w}}$ is analogous. Any input–direction different from $\underline{\mathbf{w}}$ and $\bar{\mathbf{w}}$ will lead to an amplification greater than $\underline{\sigma}$ and smaller than $\bar{\sigma}$.

Fig.1a illustrates this interpretation for the two–input/two–output case at a frequency ω^*. The input amplitude is normalised to 1. Exciting the system with inputs of varying input–direction $\alpha_u = \arctan\left(\frac{|u_2|}{|u_1|}\right)$[1] results in outputs which also have different directions (that are defined accordingly). Varying the input–direction by 360° results in a variation in the output–direction also by

[1] α_u of $\bar{\mathbf{w}}$ may have negative sign because it takes care of a possible phase–difference of the 180°.

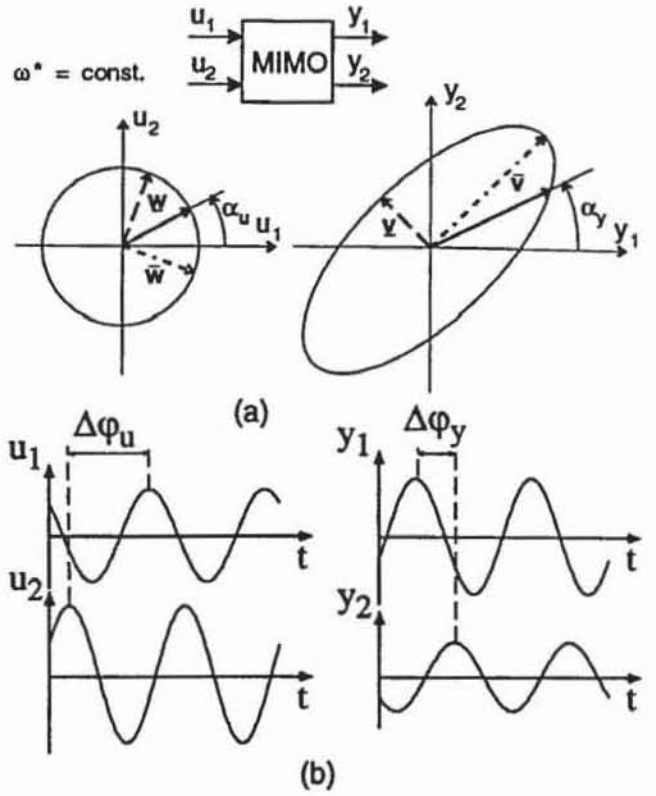

Figure 1: (a) Singular directions and (b) time–domain interpretation of phase-differences for 2×2–systems.

360°. For each input direction the gain of the system is different. Thus a circle in the input space is mapped to an ellipse in the output space. The main axis of the ellipse point into the maximal and minimal output–direction and their length is $\bar{\sigma}$ and $\underline{\sigma}$, respectively. Since for any frequency we can draw such an input phase diagram and an output ellipse we will refer to it as *dynamic* singular directions. In higher dimensional input and output spaces a frequency dependent higher dimensional input sphere and output ellipsoidal will result.

Now, we consider the general case with $\mathbf{V}$ and $\mathbf{W}$ complex. The minimal and maximal input and output–directions are now complex vectors that can be written as

$$\bar{\mathbf{w}} = \left[|\bar{w}_1| \cdot e^{j\varphi_{\bar{w}_1}}, \ldots, |\bar{w}_m| \cdot e^{j\varphi_{\bar{w}_m}}\right]^T, \text{ etc.} \qquad (2)$$

The magnitudes of the elements of $\bar{\mathbf{w}}$, $\underline{\mathbf{w}}$, $\bar{\mathbf{v}}$, and $\underline{\mathbf{v}}$ give the same information as in the real case. In addition, phase information easily interpreted in the time domain can be explored. With ω fixed, the maximal amplification of the input is achieved if the components are signals

$$u_i = |\bar{w}_i| \cdot \sin(\omega t + \varphi_{\bar{w}_i}) \qquad (3)$$

with values $\bar{w}_i$ and $\varphi_{\bar{w}_i}$ according to (2). An analogous expression holds for the minimal amplification and for $\bar{\mathbf{v}}$, $\underline{\mathbf{v}}$.

In the two–input/two–output case (Fig.1b) we will call the difference between the phase of the first and second component of the input–vector the *input–phase–difference* ($\Delta\varphi_u = \varphi(u_2) - \varphi(u_1)$) and the difference between the phase of the output components will be

referred to as *output-phase-difference* ($\Delta\varphi_y = \varphi(y_2) - \varphi(y_1)$). The *maximal* and *minimal* quantities are denoted by $\Delta\bar{\varphi}_u$ and $\Delta\bar{\varphi}_y$, respectively. If additionally, the phase-difference between u_1 and y_1 is given over frequency, then all dynamic information about the model is contained in those quantities. This time domain interpretation permits not only the comparison of models among each other. Moreover, models can be validated through experiments on the real process with these specific sine-input signals. In Section 3, this analysis technique is applied to different distillation models. A detailed discussion of singular direction analysis can be found in [7].

3 Application to distillation models

Modeling of distillation processes for control has a long tradition in which many known methodological modeling approaches have been applied. Nonetheless, there is no single recommended technique on how to derive and to validate an adequate model for control even in the binary case.

Control of a high purity binary distillation column (column A) is chosen for illustration. A brief overview of the linear models and the nonlinear model is given in Section 3.1. In Section 3.2, the linear models are analysed and compared to the nonlinear model in order to validate them. This is also meant to show the usefulness of the validation tools presented in the previous section.

3.1 Distillation models

Modeling and control of column A has been intensively investigated, recently. Five of the models used in those studies have been compared in [5]. They are also selected here for further analysis. These are the models N_1 and N_2 that are developed from physical insight based on a rigorous nonlinear model (here called model NL). Model NL assumes constant molar overflow and neglects any fluid dynamics. Index "1" and "2" stand for a model with one and two time constants, respectively. Models F_1, F_2 are based on models N_1 and N_2, respectively, containing an additional (single) time constant that is introduced to (heuristically) describe hydrodynamic effects. Model RM is a linearisation of a nonlinear constant molar overflow model including hydrodynamics that is subsequently reduced to a second-order model.

In addition, a novel linear model is included, denoted here as model W. It is based on the qualitative dynamic behavior of distillation columns which has been identified recently as a wave propagation phenomenon [4, 8, 9]. Here, both the rectifying and the stripping section reveal separately a wave which represents the concentration profile of the light component. More specifically, position and shape of the waves quantify the holdups of the light component in each column section. In the case of disturbances in flows or in feed concentration the waves propagate with analytically determinable velocities in the two sections. The wave propagation velocities are directly related to a liquid holdup change in the two sections. The modeling approach proposed in [10] can be considered as an extension of the one in [11], where the dominant time constant is determined, among others, by the change of *one* holdup of both sections. The equations of model W break down into

$$\mathbf{Y}_f(s) = \mathbf{G}_f^s(s)\mathbf{U}(s) + \mathbf{G}_f^d(s)\mathbf{Z}(s) \quad (4)$$

$$\mathbf{Y}_p(s) = \mathbf{G}_p^s(s)\mathbf{U}(s) + \mathbf{G}_p^d(s)\mathbf{Z}(s) \quad (5)$$

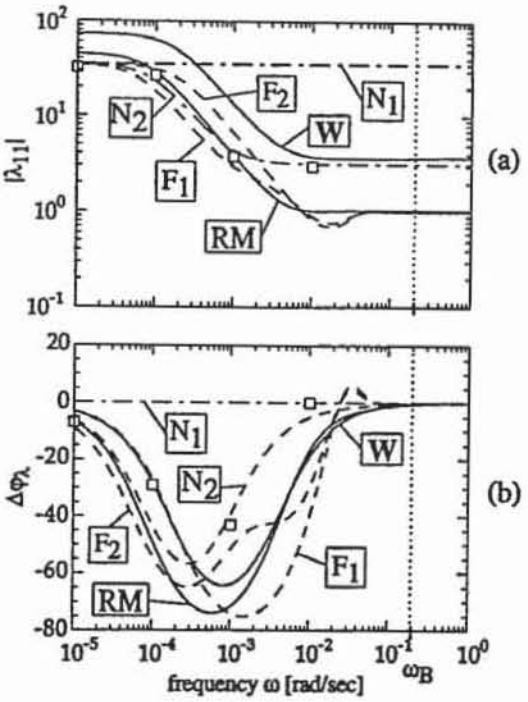

Figure 2: (a) Magnitude and (b) phase of the dynamic RGA-element λ_{11} of the models (squared points: NL).

where $\mathbf{U}(s) = [L(s), V(s)]^T$, $\mathbf{Z}(s) = [x_F(s), F(s)]^T$ $\mathbf{Y}_f(s) = [x_f^R(s), x_f^S(s)]^T$, $\mathbf{Y}_p(s) = [x^D(s), x^B(s)]^T$ and $\mathbf{G}_i^j$ being the transfer function matrices of the models. The quantities L, V, F, x_F, x^D, x^B signify the liquid and the vapor stream, and the feed rate, the feed concentration, and the top and bottom concentration, respectively. The concentrations x_f^R and x_f^S are the concentrations at the inflection point of the stationary liquid concentration profile of the rectifying and stripping section, respectively. The transfer matrices $\mathbf{G}_p^s$ and $\mathbf{G}_f^s$ are given in the Appendix. Contrary to the approaches proposed in literature, this new approach additionally provides a disturbance model ($\mathbf{G}_d^j$) consistent with the plant model ($\mathbf{G}_p^j$). In the following, the dynamic behavior of $\mathbf{G}_p^s$ of the different linear models is compared.

3.2 Validation of distillation models

We concentrate on some specific multivariable characteristics such as the dynamic relative gain array, the frequency dependent condition number, and the dynamic singular directions. A more complete treatment including the comparison of open loop responses of model NL with model W can be found in [1, 10].

RGA

Fig.2 shows magnitude and phase of the (1,1)-element $\lambda_{1,1}$ of the relative gain array for the different models. For models incorporating fluid dynamic effects (F_1, F_2, RM), the input/output channels for high frequencies are obviously decoupled as already pointed out by [5]. But also the wave model W and model N_2 show significant high frequency decoupling.

The squared point in Fig.2 correspond to the measured RGA of nonlinear model NL. The RGA is measured

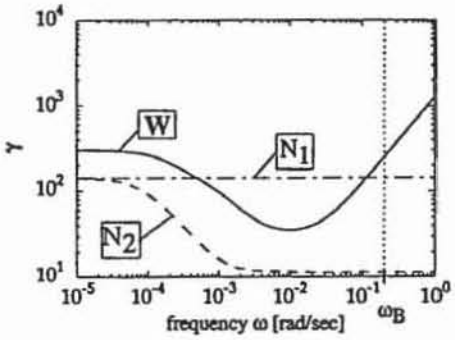

Figure 3: Condition number of linear models.

by exciting different inputs with a sinusoid of fixed frequency and amplitude. The ratio between the gain l_{11}^{u} and l_{11}^{y} (see Section 2) is the measured RGA. The regulation was achieved here with a high gain PID–controller. The gains l_{11}^{u} and l_{11}^{y} are determined by the ratio between the output and the input amplitude where in both cases the first harmonic of the Fourier series is taken. It should be noted that the measured RGA of a nonlinear system depends on the input amplitude chosen and also on the input considered for the analysis (column and row sums unequal to one). The measured RGA of model NL is very similar to the RGA of model N_2. This is not surprising, since one of the time constants of model N_2 has been fitted to the dynamic RGA (and to the singular values) [12].

In particular, high frequency decoupling is also observed for the nonlinear system without hydrodynamics as well as for models N_2 and W. This suggests that input/output decoupling for high frequencies is not only due to liquid flow delay, but it is also partly based on the different liquid holdup changes (wave velocities) in the rectifying and stripping section. This partial decoupling of the two sections relates to the fact that no fast mass exchange between the liquid holdups (large inertia) of the two sections is possible for high frequencies. High frequency excitation leads to small amplitude oscillation of the wave location. Pinched concentration profiles at the feed tray would lead to perfect decoupling. Partial decoupling, however, occurs because of non–vanishing spatial concentration gradients. For low frequencies, the waves of the two sections are almost synchronized due to the higher coupling effects caused by significant mass transfer between the rectifying and stripping section holdups. Note that perfect decoupling can be only achieved if hydrodynamics are included in the model.

CONDITION NUMBER

The condition number of models W, N_1, and N_2 is very high (Fig.3) which, together with the RGA information, suggests that distillation columns are difficult to control [12]. Model W reveals a higher condition number than models N_1 and N_2. The measured condition number of the nonlinear process is even higher for a large set of input amplitudes (compare singular direction analysis below). Contrary to models N_1 and N_2, the condition number of model W grows for high frequency. That is due to a decreasing $\underline{\sigma}$ which shows the influence of a fast pole at high frequencies. That is, $\underline{\sigma}$ decreases faster than $\bar{\sigma}$. The "additional pole" in $\underline{\sigma}$ is due to the decoupling effect in the "low–gain" direction between the two major holdups (waves) in the rectifying and stripping section

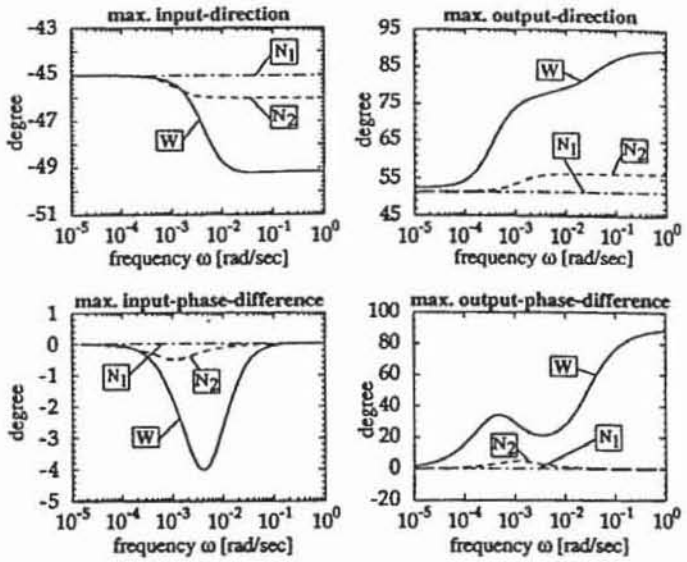

Figure 4: Extremal singular directions and phase-differences of the linear models.

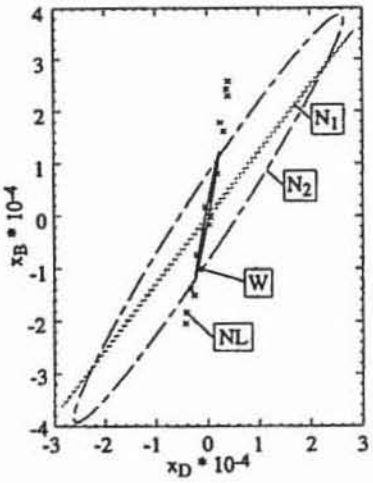

Figure 5: Ellipses of the output–directions (x^D, x^B) for models W, N_2 and the nonlinear model.

for high frequencies (compare RGA analysis).

SINGULAR DIRECTIONS

Fig.4 shows the input– and output–direction and input– and output–phase–difference of the linear models over frequency. The steady state maximal (minimal) input–direction of the models is approximately $-45°$ $(45°)$ which is in accordance with [12]. They found that for distillation columns at steady state, the most sensitive input direction is obtained by changing the external flows (e.g., $dL = -dV$), and the least sensitive input direction is obtained by changing the internal flows (e.g., $dL = dV$). In [1], another explanation based on the different wave propagation velocities in the two sections is given. For higher frequencies (more important for control), the singular directions of model W differ significantly from those of models N_1 and N_2. That is, the maximal output–direction of model W is about 40° larger than those of models N_1 and N_2. Around the envisaged bandwidth, the influence of the inputs on the bottom product concentration x^B is much stronger than on x^D. Singular directions can also be measured for nonlinear

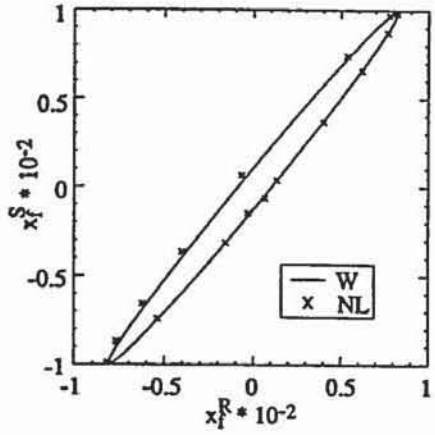

Figure 6: Ellipses of the output–directions (x_f^R, x_f^S) for model W and the nonlinear model.

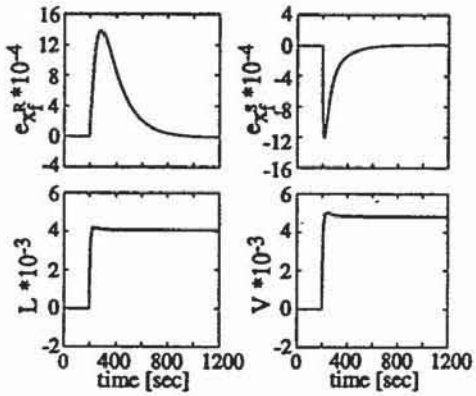

Figure 7: Responses to 15% step disturbance in F; linear (solid line) and nonlinear (dashed line) closed loop.

model NL. Fig.5 shows the output ellipses of models NL, W, N_1, and N_2 for a fixed frequency of $\omega = 10^{-2}\frac{rad}{sec}$. The extremal output–directions of the wave model almost coincide with the nonlinear model. Models N_1 and N_2 differ strongly from the nonlinear model. Furthermore, since the wave model averages process nonlinearities better than the other models, a significantly higher singular value is revealed for frequencies up to the envisaged bandwidth of the closed loop system (Fig.3 and 5). But it is much smaller than the one of the nonlinear model (Fig.5). Fig.4 shows a significanly larger maximal output–phase–difference for model W than models N_1 and N_2. Time–domain simulations (not shown) show that for higher frequencies, the maximal output–phase–difference of model W approximates best the corresponding phase of the nonlinear model. A very good correspondence of singular values and singular directions (Fig.6) can be observed between model W and the nonlinear model when concentrations at the inflection points of the stationary profiles are taken as outputs (linear model G_f^s).

4 H_∞–optimal controller design for the distillation example

Validation of different models can finally be done by controller design, if the performance of the controllers on detailed models or the real plants is compared. Since model W seems to reflect the characteristics of the non-

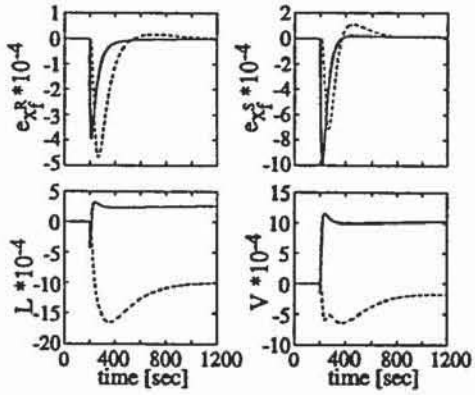

Figure 8: Responses to 15% step disturbance in x_F; linear (solid line) and nonlinear (dashed line) closed loop.

linear rigorous model best, controller design and evaluation is presented here for the wave model of column A. The (L,V)–configuration is chosen with controlled variables x_f^R and x_f^S instead of concentrations x^D and x^B. This is motivated here by the fact that singular values and singular directions of this model agree best with the nonlinear model.

H_∞–optimal controller design for this model with a mixed sensitivity criterion in which the disturbance model was explicitly taken into account is performed, leading to a dynamic compensator of order 18 that can be reduced to order 6.

Disturbances in the feed flow and feed concentration are equally well rejected with fast transient behavior and small deviations. Furthermore, no excessive action in the manipulated variables is needed. In Fig.7, time responses to a 15% step disturbance in F for both the controlled linear and nonlinear model are shown. Here, and also for step set–point changes, the step responses almost coincide. For disturbances in the feed concentration, a bigger difference, especially for the manipulated variables, can be observed (Fig.8). This is, however, not surprising, since model W does not take into account the additional small delay (in the order of $20sec$) caused by a trigger wave on the background of the concentration profile as a consequence of concentration disturbance ([8]). The different steady–states of the manipulated variables indicate that a certain separation requires only the same liquid–to–vapor ratio but not the same absolute values.

5 Conclusions

Open–loop time domain simulations of models for controller design are of minor importance since they do not expose significant differences of the linear and nonlinear models which then become evident in the closed loop [6]. In this paper, analysis tools in the frequency domain are suggested to examine the I/O–behavior of multivariable systems. The condition number and the well–known relative gain array are presented that is extended by the phase–differences of its elements. The phase–difference provides additional information about the interactions effects. Many authors suggest to examine singular values for model validation. However, singular value analysis of ill–conditioned systems can be very misleading because only partial information is included. Unlike the aforementioned tools, the proposed analysis of the dy-

	$G_f^i(s)$			
	$N_1^i(s)$	$N_2^i(s)$	$N_3^i(s)$	$N_4^i(s)$
K_j^i	753	-748	808	-812
T_1^i	4049	4049	4050	4050
T_2^i	1233	1228	1210	1210
T_3^i	220	187	221	253
T_4^i	5	5	5	5

	$G_p^i(s)$			
	$N_1^i(s)$	$N_2^i(s)$	$N_3^i(s)$	$N_4^i(s)$
K_j^i	86	-85	111	-111
T_1^i	1233	1228	4050	4050
T_2^i	220	187	221	260
T_3^i	5	5	39	38
T_4^i	+0	-0	5	5

Table 1: Transfer functions of wave model W for column A.

namic singular directions and phase–differences explores the full information about the linear dynamics. In our case study, the analysis of the magnitude of the dynamic relative gain array for models W, N_2, and NL only reveals small differences. The analysis of the condition number gives a better diversification of the models. However, the analysis of the dynamic singular directions and phase–differences is best suited to reveal significant differences between the different models for validation purpose and model discrimination especially in the frequency region in which the bandwidth is usually chosen in distillation column controller design.

The analysis of linear models W, N_1, and N_2 shows significant differences between them. Although the analysis of the RGA suggests that model N_2 approximates the nonlinear model best, the singular directions, phase–differences, and condition number of N_2 differ significantly from the ones of the nonlinear model. Hence, results from RGA analysis have to be interpreted with care. None of the linear models reflect the characteristics of the nonlinear system correctly. One exception is the wave model W with concentrations at the point of inflection of the stationary profiles chosen as outputs. Singular direction analysis reveals that only the wave model gives a good estimate for multivariable directions of the nonlinear model for higher frequencies. In general, available candidate models of the process (ideally including the real plant) should be analysed by the aforementioned tools in order to have a good decision–making basis to discriminate models for controller design, although much computation effort is necessary. Validation of the linear distillation models in this paper is based on a comparison of the model properties to those found for a rather simple nonlinear model. The same investigation (dynamic RGA, singular directions, etc.) can of course be performed for a real column or at least for a more detailed nonlinear model and its approximating linear models which include energy balances and possibly hydrodynamic effects. This is an interesting next step also in the discussion on which physical effects have to be included in a model for controller design.

Appendix

Transfer matrix data for model W are given in table 1 with

$$G_i^i(s) = \frac{1}{D(s)} \begin{bmatrix} N_1^i(s) & N_2^i(s) \\ N_3^i(s) & N_4^i(s) \end{bmatrix}$$

$$N_j^i(s) = K_j^i \prod_{k=1}^{4} (T_k^i s + 1), j = 1, \ldots, 4, \quad i \in \{f, p\}$$

and

$$D(s) = (5821s+1)(4038s+1)(1161s+1)(221s+1)(5s+1)$$

(T_j^i in $[sec]$, K_j^i in $[\frac{kmol}{sec}]$ or $[-]$) with a feed rate chosen as $F = 0.01\frac{kmol}{sec}$ and holdups as in [12].

References

[1] Amrhein M. (1992): *Diplomarbeit*, Universität Stuttgart (unpublished).

[2] Bristol E.H. (1966): " On a New Measure of Interaction for Multivariable Process Control", *IEEE Trans.Automat.Contr.*, AC–11, 133–134.

[3] Gilles, E.D. and B. Retsbach (1983): "Reduced models and control of distillation columns with sharp temperature profiles", *IEEE Trans.Aut.Control*, AC–28, 628–630.

[4] Hwang Y.–L., and H. Helfferich (1991): "Nonlinear wave theory for dynamics of binary distillation columns", *AIChE J.*37(5), 705-723.

[5] Jacobsen, E.W., P. Lundström, and S. Skogestad (1990): "Modelling requirements for robust control of distillation columns", *Proc. 11th IFAC World Congress*, Tallin, Estonia.

[6] Jacobsen, E.W. (1991): "Studies on Dynamics and Control of Distillation Columns", *PhD thesis*, 73–92, Trondheim, Norway.

[7] Kurz W. (1991): *Studienarbeit*, Universität Stuttgart (unpublished).

[8] Marquardt W. (1988): "Nichtlineare Wellenausbreitung — Ein Weg zu reduzierten dynamischen Modellen von Stofftrennprozessen", *Fortschr.–Ber. VDI Reihe 8 Nr. 161*, VDI–Verlag, Düsseldorf.

[9] Marquardt W. (1990): "Traveling waves in chemical processes" *Int.Chem.Engng.*, 30(4), 585–606.

[10] Marquardt W., and M. Amrhein (1993): "Development of a linear distillation model from design data for process control", *ESCAPE 93, 5–7 July 1993*, Graz, Austria.

[11] Skogestad S., and M. Morari (1987): "The dominant time–constant for distillation columns", *Comp.Chem.Eng.*, 11(6), 607–617.

[12] Skogestad S., and M. Morari (1988) "Understanding the dynamic behavior of distillation columns", *Ind.Eng.Chem.Res.*27, 1848–1862.

[13] Skogestad S.: "Robust control", In W.L. Luyben, ed., *Practical Distillation Control*, Chapter 14, to appear.